GDCh

**Communications**

*Angewandte*
*Chemie*
International Edition
www.angewandte.org

**Cluster Compounds** | Hot Paper

# Siliconoid Expansion by a Single Germanium Atom through Isolated Intermediates

*Nadine E. Poitiers, Volker Huch, Bernd Morgenstern, Michael Zimmer, and David Scheschkewitz\**

Dedicated to Professor Holger Braunschweig on the occasion of his 60th birthday

**Abstract:** The growth of (semi-)metal clusters is pivotal for nucleation processes in gaseous and condensed phases. We now report the isolation of intermediates during the expansion of a stable unsaturated silicon cluster (siliconoid) by a single germanium atom through a sequence of substitution, rearrangement and reduction. The reaction of *ligato*-lithiated hexasilabenzpolarene LiSi$_6$Tip$_5$ (**1**Li·(thf)$_2$, Tip = 2,4,6-triisopropylphenyl) with GeCl$_2$·NHC (NHC = 1,3-diisopropyl-4,5-dimethylimidazol-2-ylidene) initially yields the product with exohedral germanium(II) functionality, which then inserts into an Si–Si bond of the Si$_6$ scaffold. The concomitant transfer of the chloro functionality from germanium to an adjacent silicon preserves the electron-precise nature of the formed endohedral germylene. Full incorporation of the germanium heteroatom to the Si$_6$Ge cluster core is finally achieved either by reduction under loss of the coordinating NHC or directly by reaction of **1**Li·(thf)$_2$ with GeCl$_2$·1,4-dioxane.

**M**etal and semi-metal clusters are key intermediates of the deposition of nanostructures (particles, wires and films) as well as bulk materials.[1] Unsaturated silicon clusters (siliconoids)[2] are particularly noteworthy due to the prominent role of silicon in pivotal technologies of modern society. According to our definition,[3] siliconoids feature one or more unsubstituted vertices with hemispheroidal coordination environment, which resemble the free valencies of bulk and nanoscalar silicon surfaces.[4]

The first stable siliconoid Si$_5$R$_6$ was reported in 2005[5] and followed by numerous further examples.[6,7] Since recently, anionic siliconoids have become available, either through reductive cleavage of substituents from neutral

siliconoids[7c,8] or the grafting of substituents to unsubstituted deltahedral Zintl anions by treatment with suitable electrophiles.[6j,k,9,10] Anionic siliconoids constitute valuable starting materials for the incorporation of further functionality and heteroatoms[11] as well as the atomically precise expansion of the cluster scaffold by reaction with SiCp*$_2$ and a subsequent reduction step, which constitutes a systematic model for the growth of transient silicon clusters.[7c] While in case of Zintl anions[12] and metalloids[13] of germanium and tin, binary systems containing heteroatoms are well established, the number of heteronuclear siliconoids is limited.[14] Aside from a silyl-substituted germanium-rich Ge$_{10}$Si anion,[14a] only a few heterosiliconoids of the Si$_4$Ge$_2$ and Si$_4$Sn$_2$ type are known,[14d] which can also be selectively lithiated in case of Si$_4$Ge$_2$.[14e] In view of the technological importance of Ge-doped bulk silicon-based materials,[15] we contemplated the possibility of atomically precise Ge-doping at the molecular level.

Herein, we report the reactions of *ligato*-lithiated hexasilabenzpolarene **1**Li·(thf)$_2$ with NHC- and 1,4-dioxane-coordinated GeCl$_2$ (NHC = 1,3-diisopropyl-4,5-dimethylimidazol-2-ylidene; for a definition of the prefixes for unambiguous identification of the four distinct positions in benzpolarenes, the assumed global minimum isomers of E$_6$H$_6$ for E = Si, Ge, Sn, see ref. [2a, 8b]). By variation of the conditions, we obtained different products with a variable extent of incorporation of the single Ge atom into the cluster scaffold thus providing a series of isolable intermediates of this fundamental process of cluster growth.

In a preliminary NMR scale reaction of **1**Li·(thf)$_2$ with one equivalent of GeCl$_2$·NHC at −78 °C, a few red crystals were collected and investigated by X-ray diffraction[16] showing a dimeric structure of the thf-adduct of the exohedrally germylene-functionalized hexasilabenzpolarene **2** (Scheme 1, Figure 1). As the two major products of the otherwise complex reaction mixture contained coordinated NHC according to $^{13}$C and $^1$H NMR data, the dimer [**2**·thf]$_2$ apparently represents a spectroscopically undetected minor component. The structure of [**2**·thf]$_2$ contains two uncompromised Si$_6$ benzpolarene scaffolds connected by a planar four-membered Ge$_2$Cl$_2$ ring with to Ge-coordinating thf molecules. The low quality of the data set due to weakly diffracting crystals prevents us from a discussion beyond connectivity. Unfortunately, the isolated amount of [**2**·thf]$_2$ was insufficient for further characterization or repeated crystallization.

[*] Dr. N. E. Poitiers, Dr. V. Huch, Dr. B. Morgenstern, M. Zimmer, Prof. Dr. D. Scheschkewitz
Krupp Chair in General and Inorganic Chemistry, Saarland University (Germany)
E-mail: scheschkewitz@mx.uni-saarland.de
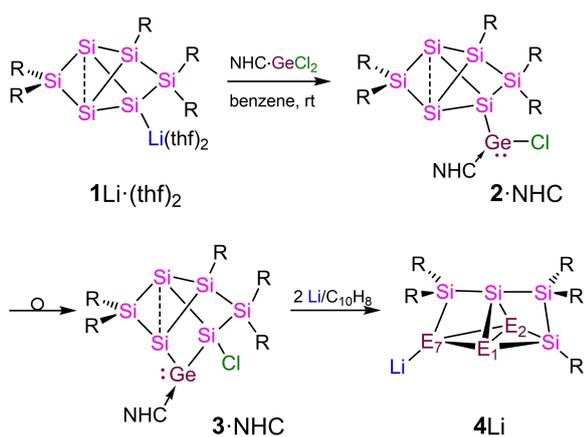
**Scheme 1.** Siliconoid expansion via **2**·NHC and **3**·NHC by reaction of **1**Li·(thf)$_2$ with GeCl$_2$·NHC (NHC = 1,3-diisopropyl-4,5-dimethylimidazol-2-ylidene) and reductive scrambling of Ge position to yield **4**Li (**4**: E$_1$ = Si, E$_2$ = Si, E$_7$ = Ge; **4'**: E$_1$ = Ge, E$_2$ = Si, E$_7$ = Si; **4''**: E$_1$ = Si, E$_2$ = Ge, E$_7$ = Si; R = Tip = 2,4,6-triisopropylphenyl).
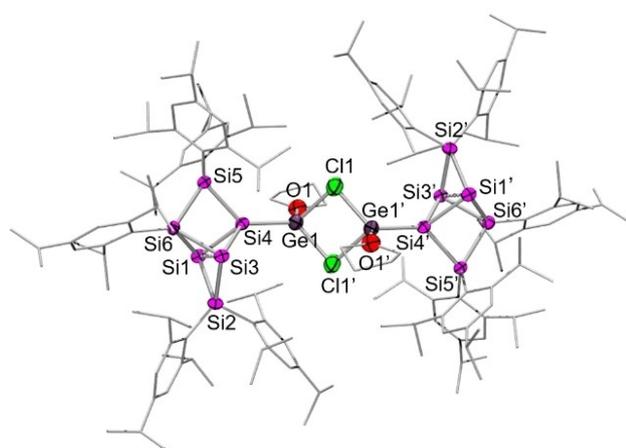


**Figure 1.** Molecular structure of [**2**·thf]$_2$ in the solid state. H atoms omitted for clarity. Ellipsoids at 50%. Due to the mediocre quality of the data set bonding parameters are not discussed.

On a preparative scale, **1**Li·(thf)$_2$ was treated with NHC·GeCl$_2$ in benzene at room temperature. Only the two major components of the NMR scale reaction were obtained in this case. They show a somewhat less wide distribution of $^{29}$Si NMR signals than typically observed for uncompromised hexasilabenzpolarene scaffolds (minor product: +97.6 to −204.1 ppm; major product: +69.5 to −189.5 ppm). The different solubilities allow for the separation of the mixture through extraction/crystallization sequences: washing with hexane transfers the major component into the filtrate, while the minor is isolated as red microcrystalline powder in 20% yield by extraction of the solid residue with benzene and subsequent precipitation from toluene. All attempts to grow single crystals of the tentative initial product **2**·NHC, however, led to its rearrangement to the major component, **3**·NHC (Scheme 1).

Reaction of the *ligato*-lithiated siliconoid **1**Li·(thf)$_2$ with 1.1 equivalents of NHC·GeCl$_2$ in benzene at 60°C indeed

results in the exclusive formation of **3**·NHC after 15 h, which was isolated as dark-red crystals from hexane in 77% yield. The $^{29}$Si NMR spectrum in C$_6$D$_6$ shows six signals at 69.5, 21.7, 19.6, −39.2, −188.5, and −189.5 ppm. Although the retention of two unsubstituted vertices is apparent from the presence of the two highfield signals, the significantly less wide distribution of $^{29}$Si NMR shifts than in uncompromised hexasilabenzpolarenes suggested structural alterations compared to the initial substitution product **2**·NHC.[7b,c,8,11b,c]

X-ray diffraction on single crystals[16] obtained at room temperature from a concentrated benzene solution (Figure 2) indeed revealed the constitution of **3**·NHC as insertion product of the exohedral germylene moiety of the plausible intermediate **2**·NHC into the adjacent Si3–Si4 single bond of the Si$_6$ scaffold. The chloro ligand is concomitantly transferred from germanium to the former *ligato*-vertex Si4. The very similar CP-MAS NMR data of a crystalline sample support the near-identity of structures in the solid state and in solution. The cluster core exhibits a propellane-like motif with two unsubstituted vertices in hemispheroidal coordination environments (Si1 and Si3). The NHC-coordinated Ge$^{II}$ center—due to its electronically saturated nature—can be regarded as a simple electron-precise expansion of one of the three-membered rings of the hexasilabenzpolarene motif to a four-membered ring. Apparently, the coordination of the NHC prevents a full endohedral incorporation such as the one previously reported for the formation of an Si$_7$ siliconoid.[7c] The distance between the unsubstituted vertices (Si1–Si3 2.598(2) Å) in **3**·NHC is slightly shorter than in *ligato*-substituted Si$_6$ benzpolarenes or Breher's pentasilapropellane (2.6176 to 2.6598 Å)[6b,7b,8] and comparable to *ligato*-metallocene substituted siliconoids (2.588 Å).[11b] The two Ge–Si bonds differ considerably (Ge1–Si3 2.480(2) Å; Ge1–Si4 2.365(2) Å), which may be a consequence of donation of electron density
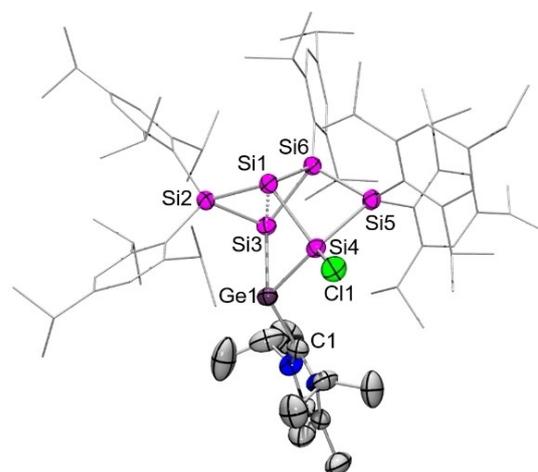


**Figure 2.** Molecular structure of **3**·NHC in the solid state. Aryl groups displayed as wireframes. Hydrogen atoms omitted for clarity. Thermal ellipsoids at 50%. Selected bond lengths [Å] and angles [°]: Ge1–C1 2.030(5), Ge1–Si4 2.397(1), Ge1–Si3 2.465(1), Si1–Si3 2.631(2), Si1–Si4 2.358(2); C1-Ge-Si4 113.7(1), C1-Ge-Si3 108.2(1), Si4-Ge-Si3 79.18(4).

from the lone pair at the germanium center into σ* orbitals at the Cl-substituted Si4.

In order to support the thermodynamic feasibility of the proposed rearrangement, we optimized the electronic structures of the exohedral GeCl-substituted siliconoid **2**·NHC and the endohedral germylene-expanded siliconoid **3**·NHC at the BP86-D3(BJ)/def2-SVP level of theory (Supporting Information).[17,18] Although DFT methods are known to significantly overestimate bond lengths in strongly correlated systems,[19] the experimental topology of **3**·NHC is qualitatively well reproduced and we assume that this systematic error is canceled when comparing energies. The insertion product **3**·NHC is indeed favored by $\Delta G = -17\,\text{kcal}\,\text{mol}^{-1}$. Although meaningful computations of the reaction pathway are economically out of reach due to the size of the involved molecules, the frontier orbitals of **2**·NHC are predisposed for the rearrangement to **3**·NHC. The HOMO of **2**·NHC represents the lone pair at the germanium atom, while the LUMO exhibits major contributions at the *privo* and *nudo* vertices, allowing for either an intra- or intermolecular attack of the latter by the former (Figure 3).

UV/Vis monitoring of the isolated initial substitution product of alleged constitution **2**·NHC in hexane at 60 °C during approximately 6 h shows the gradual appearance of
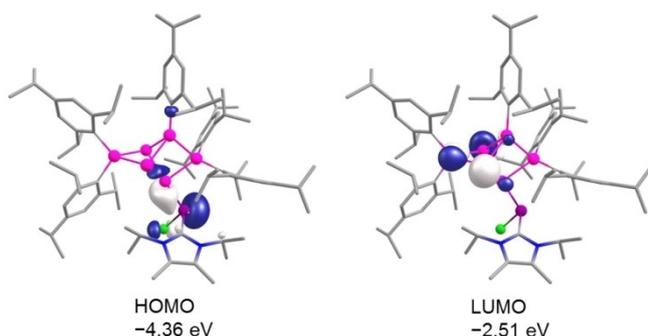


HOMO
−4.36 eV

LUMO
−2.51 eV

***Figure 3.*** Frontier molecular orbitals of exohedrally germylene-substituted **2**·NHC at the BP86-D3(BJ)/def2-SVP level of theory (isocontour value at 0.052).
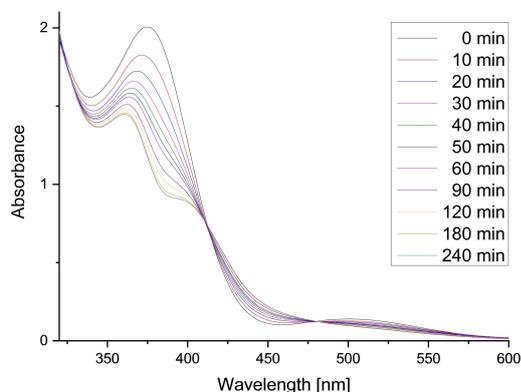


***Figure 4.*** UV/Vis monitoring of the electron-precise cluster expansion from exohedral germylene **2**·NHC to **3**·NHC ($10^{-6}\,\text{mol}\,\text{L}^{-1}$, 60 °C).

bands at 360 and 383 nm at the expense of those at 375 nm (Figure 4). Two isosbestic points at 479 and 411 nm (within the margin of error; additional isobestic points in the UV are obscured as the responsible ligand-centered absorptions do not change by much; see Figure S16) suggest the absence of secondary reaction paths and thus confirm the uniformity of the rearrangement to the endohedral siliconoid **3**·NHC as observed by NMR spectroscopy. Extended heating to 60 °C after completed conversion to **3**·NHC leads to a slight decrease of the absorption bands suggesting minor decomposition at high dilution, presumably due to trace oxygen or moisture. At the higher concentrations of NMR samples, **3**·NHC is stable in $C_6D_6$ solution for at least several days under argon. The experimental UV/Vis absorption bands of **2**·NHC and **3**·NHC are in satisfactory agreement with the TD-DFT calculations at the BP86-D3(BJ)/def2-SVP level of theory (see Supporting Information). The calculated longest wavelength absorption band of **2**·NHC at $\lambda_{\text{max,calc}} = 517$ nm is slightly red shifted compared to the experimental value of $\lambda_{\text{max,exp}} = 504$ nm. It consists predominantly of the HOMO−1→LUMO transition (80 %). The longest wavelength absorption of the expansion product with electron-precise endohedral germylene moiety, **3**·NHC, at $\lambda_{\text{max}} = 511$ nm is red-shifted to $\lambda_{\text{max,calc}} = 536$ nm in the calculated spectrum as well and is almost exclusively due to the HOMO→LUMO transition (91 %).

Inspired by the previously reported synthesis of $Si_7Tip_5Li$,[7c] we attempted the reduction of **3**·NHC with 2.2 equivalents of lithium/ naphthalene in order to completely incorporate the germanium center into the delocalized cluster core of a lithiated 7-vertex cluster **4**Li (Scheme 1). Liberated NHC was removed by crystallization from a mixture of hexane/dme. The $^{29}$Si NMR of the thus obtained product mixture with dme as only external donor indeed shows very similar chemical shifts (from 358.0 to −193.8 ppm) as those of $Si_7Tip_5Cp^*$.[7c] The signals are grouped in seven sets, four of which consist of three signals each and the remaining three of just two. The lack of a third signal in the latter is plausibly explained by partial occupation of the corresponding vertices by germanium, suggesting the presence of three positional isomers **4**, **4′** and **4″** (Scheme 1, Figure 5). For mixed Si/Ge Zintl anions a statistical scrambling of the germanium positions over the entire polyhedral cluster has been reported.[12] Indeed, none of the signal sets associated to germanium-doped vertices shows cross-peaks in the 2D $^{29}$Si/$^1$H correlation NMR spectrum, which are thus identified as unsubstituted. While the signals at −193.8, 189.8, −142.3 and −139.4 ppm are assigned to either of the vertices E1 and E2, the two extremely deshielded signals at 358.0 and 353.1 ppm are due to the tetracoordinate (!) lithiated vertex E7 according to the substantial line broadening through coupling to the quadrupolar $^7$Li nucleus ($\delta^7\text{Li} = -0.978$ ppm). This lowfield shift exceeds the $^{29}$Si-deshielding of the lithiated *privo*-vertex of an $Si_6$ siliconoid by almost 100 ppm ($\delta^{29}\text{Si} = 267.9$ ppm).[8b] An additional group of three signals at −61.4, −64.0 and −66.0 ppm without cross-peaks in the $^{29}$Si/$^1$H correlation is indicative of the presence of yet another unsubstituted silicon vertex albeit without germanium incorporation. All
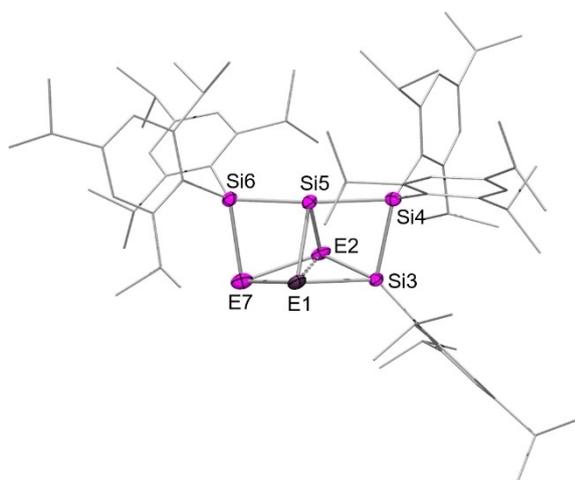
**Figure 5.** Molecular structure of the anion of solvent-separated ion pair of siliconoid **4[Li·(dme)₂]** in the solid state. Aryl groups displayed as wireframes. Hydrogen atoms and [Li(dme)₂]⁺ omitted for clarity. Thermal ellipsoids at 50%. The different Si/Ge occupations **4**, **4′** and **4″** were refined as a split model, but only the major occupation **4** is displayed. (**4**: E₁ = Si, E₂ = Si, E₇ = Ge; **4′**: E₁ = Ge, E₂ = Si, E₇ = Si; **4″**: E₁ = Si, E₂ = Ge, E₇ = Si). Relevant bond lengths cannot reliably be discussed due to the mixed occupation.

three germanium positions are refined to 52% (**4**), 21% (**4′**) and 27% (**4″**) for **4Li·(NHC)₂** and 41% (**4**), 27% (**4′**) and 32% (**4″**) for **4[Li·(dme)₂]**, which is approximately identical to the values in solution within the margin of error.

In order to exclude that the formation of [**2·thf**]₂ is due to residual traces of GeCl₂·1,4-dioxane in the NHC·GeCl₂ precursor, we deliberately treated siliconoid **1Li·(thf)₂** with one equivalent of GeCl₂·1,4-dioxane in thf at −80°C (Scheme 2). The obtained reaction mixture reveals the wide dispersion of chemical shifts in the ²⁹Si NMR that is typical of exohedrally functionalized hexasilabenzpolarenes. The presence of seven groups of signals between +182.1 and −241.1 ppm with either two or three resonances each, however, suggested the scrambling of germanium over several positions as observed for **4**. In this light, the expansion of the cluster core by the germanium center seemed likely although the applied 1:1 stoichiometry clearly excluded the complete elimination of the Ge-bonded chlorine.

X-ray diffraction on single crystals[16] confirmed the endohedral incorporation of the germanium atom in the neutral Si₆Ge heterosiliconoid **5** with three positional isomers **5**, **5′** and **5″** (Figure 6). The cluster core resembles

other signals are observed at unremarkable chemical shifts as sets of three signals and are thus assigned to either SiTip₂ or SiTip units. Therefore, the fully incorporated germanium atom occupies either of the three hemispheroidal vertices in **4Li**, but not the position with the unusual see-saw coordination (Si5, see below).
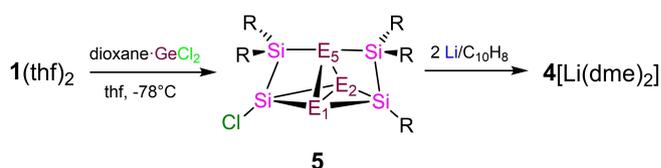
In the CP-MAS ²⁹Si NMR, crystalline samples of **4[Li·(dme)₂]** show three sets of six ²⁹Si resonances from +323.3 ppm to −191.5 ppm (Table 2, see Supporting Information for details) implying the subsistence of the positional isomers **4**, **4′** and **4″** in the solid state. Single-crystal X-ray diffraction analyses[16] of both the contact ion pair of **4Li·(NHC)₂** and solvent-separated ion pair of **4[Li(dme)₂]** were obtained by crystallization in 40% (**4Li·(NHC)₂** from hexane; see Supporting Information) and 61% yields (**4[Li·(dme)₂]** from hexane/dme) and confirmed the distribution of germanium over three different hemispheroidal vertices of the rearranged Si₆Ge scaffold (Figure 5).

As the mixed occupation of the germanium atom does not allow for a discussion of parameters involving germanium, we restrict the following section to the unaffected parts of the heterosiliconoid. The cluster core of **4[Li(dme)₂]** exhibits a propellane motif distorted by the twofold interconnection of the "propeller blades", similar to Si₇Tip₅Cp* and Si₇Tip₅Li.[7c] This results in a seesaw-type coordination environment at Si5 with a quasi-linear arrangement with respect to Si6 and Si4 (Si6–Si5–Si4 of **4[Li(dme)₂]**: 173.52-(3)°, Si6–Si5–Si4 of **4Li·(NHC)₂**: 176.50(2)° vs 173.77° for Si₇Tip₅Cp* and 162.705(4)° for Si₇E).[7c,11d] While the two basal vertices of the central triangular motif, E1 and E2, as well as the formally anionic vertex E7 are either occupied by silicon or germanium, position 5 only by silicon confirming the conclusions from ²⁹Si NMR. The relative occupations of



**Scheme 2.** Siliconoid expansion by germanium with GeCl₂·dioxane to mixture of positional isomers **5** (**5**: E₁ = Si, E₂ = Si, E₅ = Ge; **5′**: E₁ = Ge, E₂ = Si, E₅ = Si; **5″**: E₁ = Si, E₂ = Ge, E₅ = Si; R = Tip = 2,4,6-triisopropyl-phenyl).
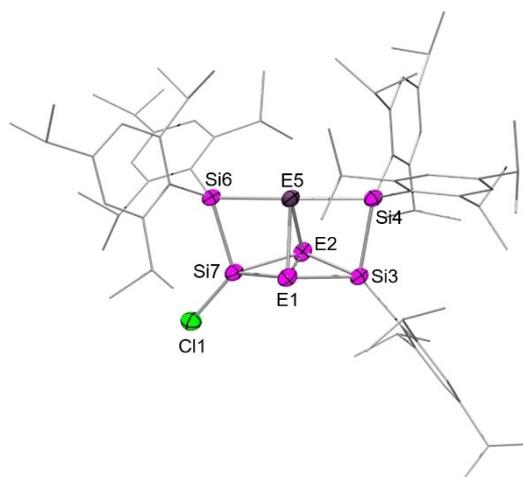


**Figure 6.** Molecular structure of the major positional isomer of **5**. Aryl groups displayed as wireframes. Hydrogen atoms omitted for clarity. Thermal ellipsoids at 50%. The different Si/Ge occupations **5**, **5′** and **5″** were refined as a split model, but only the major occupation **5** is displayed. (**5**: E₁ = Si, E₂ = Si, E₅ = Ge; **5′**: E₁ = Si, E₂ = Ge, E₅ = Si; **5″**: E₁ = Ge, E₂ = Si, E₅ = Si). The most relevant bond lengths cannot reliably be discussed due to the mixed occupation.

that of anionic heterosiliconoid **4**[Li(dme)$_2$] with the twofold interconnection between the "propeller blades" leading to a seesaw-type coordination environment at E5. In contrast to **4**[Li(dme)$_2$] and **4**Li·(NHC)$_2$, however, the germanium atom is distributed over base and apex of the central triangular motif (E1, E2, E5), while the functionalized vertex is occupied by silicon exclusively (Si7). The occupations of the three germanium positions were refined to 52% (**5**), 21% (**5′**) and 27% (**5″**) in the solid state.

In C$_6$D$_6$ solution, three sets of two signals each in the highfield region without cross-peak in the 2D $^{29}$Si/$^1$H correlation NMR spectrum are attributed to unsubstituted vertices, which—in this case—correspond to base and apex of the central triangle, E1, E2 and E5. The two less intense signals at −157.2 and −157.3 ppm are assigned to the silicon atoms in position E5 of the formally enantiomeric species **5′** and **5″**, which can be distinguished NMR-spectroscopically due to the discrimination through desymmetrization by the rotationally hindered ligand periphery. The more intense signals at −225.7 and −241.1 ppm are due to E1 and E2 of isomer **5** and the less intense signals at −213.6 and −224.6 ppm arise from the isomers **5′** and **5″**, each with only one Si atom at these two positions. The group of three signals at 138.4, 135.1 and 110.1 ppm is assigned to the chlorinated silicon vertex Si7 based on the absence of a cross-peak in the $^{29}$Si/$^1$H-correlated NMR spectrum. The remaining three sets of three signals each are attributed to SiTip or SiTip$_2$ vertices. The CP-MAS $^{29}$Si NMR of the isolated crystals of **5** is consistent with the signals observed in solution, albeit some are too close to be resolved (Supporting Information).

Reduction of the isomeric mixture of **5** was expected to provide an alternative access to the anionic **4**[Li·(dme)$_2$]. We therefore treated **5** with 2.2 equivalents of lithium/naphthalene. Indeed, the $^{29}$Si NMR of the crude product shows approximately the same chemical shifts as discussed for **4**[Li·(dme)$_2$]. Notably, the germanium positions change in the course of the reaction from E1, E2, and E5 in **5** to E1, E2, and E7 in **4**[Li·(dme)$_2$] in similar ratios as obtained by reduction of **3**·NHC, which strongly suggests that the cluster scaffold is intermittently opened to an exohedrally functionalized short-lived intermediate of unknown identity in the course of the reduction.

In conclusion, the expansion of the Si$_6$ benzpolarene scaffold by a single germanium atom can be arrested at different stages through the stabilization of otherwise fleeting intermediates by the coordination of an NHC to the electron-deficient germanium center. In this manner, we characterized the exohedrally germylene-functionalized benzpolarene **2**·NHC and the electron-precise insertion product **3**·NHC. While in this case, the cleavage of the NHC (and with that full endohedral incorporation of the germanium atom to **4**[Li(dme)$_2$]) is only achieved upon reductive chloride elimination, the reaction of GeCl$_2$·1,4-dioxane with the *ligato*-lithiated hexasilabenzpolarene **1**Li·(thf)$_2$ directly affords the isomeric mixture of **5** with the germanium atom fully incorporated into the cluster core.

## Conflict of Interest

The authors declare no conflict of interest.

## Data Availability Statement

The data that support the findings of this study are available in the Supporting Information of this article.

[1] e.g. a) N. Cheng, S. Stambula, D. Wang, M. N. Banis, J. Liu, A. Riese, B. Xiao, R. Li, T.-K. Sham, L.-M. Liu, G. A. Botton, X. Sun, *Nat. Commun.* **2016**, *7*, 13638; b) S. Stavrić, M. Belić, Z. Šljivančanin, *Carbon* **2016**, *96*, 216–222; c) M. R. Friedfeld, J. L. Stein, B. M. Crossairt, *Inorg. Chem.* **2017**, *56*, 8689–8697.

[2] a) Y. Heider, D. Scheschkewitz, *Chem. Rev.* **2021**, *121*, 9674–9718; b) Y. Heider, D. Scheschkewitz, *Dalton Trans.* **2018**, *47*, 7104–7112; c) S. Kyushin, *Organosilicon Compounds, Vol. 1* (Ed.: V. Y. Lee), Academic Press, New York, **2017**, chap. 3; d) T. Iwamoto, S. Ishida, *Chem. Lett.* **2014**, *43*, 164–170.

[3] K. Abersfelder, A. Russell, H. S. Rzepa, A. J. P. White, P. R. Haycock, D. Scheschkewitz, *J. Am. Chem. Soc.* **2012**, *134*, 16008–16016.

[4] H. Neergaard Waltenburg, J. T. Yates, Jr., *Chem. Rev.* **1995**, *95*, 1589–1673.

[5] D. Scheschkewitz, *Angew. Chem. Int. Ed.* **2005**, *44*, 2954–2956; *Angew. Chem.* **2005**, *117*, 3014–3016.

[6] a) G. Fischer, V. Huch, P. Mayer, S. K. Vasisht, M. Veith, N. Wiberg, *Angew. Chem. Int. Ed.* **2005**, *44*, 7884–7887; *Angew. Chem.* **2005**, *117*, 8096–8099; b) D. Nied, R. Köppe, W. Klopper, H. Schnöckel, F. Breher, *J. Am. Chem. Soc.* **2010**, *132*, 10264–10265; c) A. Tsurusaki, C. Iizuka, K. Otsuka, S. Kyushin, *J. Am. Chem. Soc.* **2013**, *135*, 16340–16343; d) A. Tsurusaki, J. Kamiyama, S. Kyushin, *J. Am. Chem. Soc.* **2014**, *136*, 12896–12898; e) T. Iwamoto, N. Akasaka, S. Ishida, *Nat. Commun.* **2014**, *5*, 5353; f) N. Akasaka, S. Ishida, T. Iwamoto, *Inorganics* **2018**, *6*, 107; g) J. Keuter, K. Schwedtmann, A. Hepp, K. Bergander, O. Janka, C. Doerenkamp, H. Eckert, C. Mück-Lichtenfeld, F. Lips, *Angew. Chem. Int. Ed.* **2017**, *56*, 13866–13871; *Angew. Chem.* **2017**, *129*, 14054–14059; h) K. Schwedtmann, A. Hepp, K. Schwedtmann, J. J. Weigand, F. Lips, *Eur. J. Inorg. Chem.* **2019**, 4719–4726; i) J. Keuter, C. Schwermann, A. Hepp, K. Bergander, J. Droste, M. R. Hansen, N. L. Doltsinis, C. Mück-Lichtenfeld, F. Lips, *Chem. Sci.* **2020**, *11*, 5895–5901; j) L. J. Schiegerl, A. J. Karttunen, W. Klein, T. F. Fässler, *Chem. Eur. J.* **2018**, *24*, 19171–19174;

k) L. J. Schiegerl, A. J. Karttunen, W. Klein, T. F. Fässler, *Chem. Sci.* **2019**, *10*, 9130–9139.

[7] a) K. Abersfelder, A. J. P. White, H. S. Rzepa, D. Scheschke-witz, *Science* **2010**, *327*, 564–566; b) K. Abersfelder, A. J. P. White, R. J. F. Berger, H. S. Rzepa, D. Scheschkewitz, *Angew. Chem. Int. Ed.* **2011**, *50*, 7936–7939; *Angew. Chem.* **2011**, *123*, 8082–8086; c) K. I. Leszczyńska, V. Huch, C. Präsang, J. Schwabedissen, R. J. F. Berger, D. Scheschkewitz, *Angew. Chem. Int. Ed.* **2019**, *58*, 5124–5128; *Angew. Chem.* **2019**, *131*, 5178–5182.

[8] a) P. Willmes, K. Leszczyńska, Y. Heider, K. Abersfelder, M. Zimmer, V. Huch, D. Scheschkewitz, *Angew. Chem. Int. Ed.* **2016**, *55*, 2907–2910; *Angew. Chem.* **2016**, *128*, 2959–2963; b) Y. Heider, N. E. Poitiers, P. Willmes, K. I. Leszczyńska, V. Huch, D. Scheschkewitz, *Chem. Sci.* **2019**, *10*, 4523–4530.

[9] a) C. Lorenz, F. Hastreiter, K. Hioe, N. Lokesh, S. Gärtner, N. Korber, R. M. Gschwind, *Angew. Chem. Int. Ed.* **2018**, *57*, 12956–12960; *Angew. Chem.* **2018**, *130*, 13138–13142; b) T. Henneberger, W. Klein, T. F. Fässler, *Z. Anorg. Allg. Chem.* **2018**, *644*, 1018–1027; c) F. Hastreiter, C. Lorenz, J. Hioe, S. Gärtner, N. Lokesh, N. Korber, R. M. Gschwind, *Angew. Chem. Int. Ed.* **2019**, *58*, 3133–3137; *Angew. Chem.* **2019**, *131*, 3165–3169.

[10] Very recent reviews on Zintl anions in solution: a) Y. Wang, J. E. McGrady, Z.-M. Sun, *Acc. Chem. Res.* **2021**, *54*, 1506–1516; b) J. E. McGrady, F. Weigend, S. Dehnen, *Chem. Soc. Rev.* **2022**, *51*, 628–649; c) M. Schütz, C. Gemel, W. Klein, R. A. Fischer, T. F. Fässler, *Chem. Soc. Rev.* **2021**, *50*, 8496–8510; d) C. Liu, Z.-M. Sun, *Coord. Chem. Rev.* **2019**, *382*, 32–56; e) K. Mayer, J. Weßing, T. F. Fässler, R. A. Fischer, *Angew. Chem. Int. Ed.* **2018**, *57*, 14372–14393; *Angew. Chem.* **2018**, *130*, 14570–14593; f) R. J. Wilson, B. Weinert, S. Dehnen, *Dalton Trans.* **2018**, *47*, 14861–14869.

[11] a) Y. Heider, P. Willmes, V. Huch, M. Zimmer, D. Scheschke-witz, *J. Am. Chem. Soc.* **2019**, *141*, 19498–19504; b) N. E. Poitiers, L. Giarrana, K. I. Leszczyńska, V. Huch, M. Zimmer, D. Scheschkewitz, *Angew. Chem. Int. Ed.* **2020**, *59*, 8532–8536; *Angew. Chem.* **2020**, *132*, 8610–8614; c) N. E. Poitiers, L. Giarrana, V. Huch, M. Zimmer, D. Scheschkewitz, *Chem. Sci.* **2020**, *11*, 7782–7788; d) N. E. Poitiers, V. Huch, M. Zimmer, D. Scheschkewitz, *Chem. Eur. J.* **2020**, *26*, 16599–16602.

[12] a) S. Scharfe, F. Kraus, S. Stegmaier, A. Schier, T. F. Fässler, *Angew. Chem. Int. Ed.* **2011**, *50*, 3630–3670; *Angew. Chem.* **2011**, *123*, 3712–3754; b) M. Waibel, G. Raudaschl-Sieber, T. F. Fässler, *Chem. Eur. J.* **2011**, *17*, 13391–13394; c) M. Waibel, T. F. Fässler, *Inorg. Chem.* **2013**, *52*, 5861–5866.

[13] a) L. R. Sita, *Acc. Chem. Res.* **1994**, *27*, 191–197; b) B. E. Eichler, P. P. Power, *Angew. Chem. Int. Ed.* **2001**, *40*, 796–797;

*Angew. Chem.* **2001**, *113*, 818–819; c) A. Sekiguchi, Y. Ishida, Y. Kabe, M. Ichinohe, *J. Am. Chem. Soc.* **2002**, *124*, 8776–8777; d) A. Schnepf, *Chem. Soc. Rev.* **2007**, *36*, 745–758; e) C. Schenk, F. Henke, A. Schnepf, *Angew. Chem. Int. Ed.* **2013**, *52*, 1834–1838; *Angew. Chem.* **2013**, *125*, 1883–1887; f) C. P. Sindlinger, L. Wesemann, *Chem. Sci.* **2014**, *5*, 2739–2746; g) O. Kysliak, C. Schrenk, A. Schnepf, *Angew. Chem. Int. Ed.* **2016**, *55*, 3216–3219; *Angew. Chem.* **2016**, *128*, 3270–3274; h) M. Binder, C. Schrenk, A. Schnepf, *Chem. Commun.* **2019**, *55*, 12148–12151.

[14] a) A. Schnepf, *Chem. Commun.* **2007**, 192–194; b) D. Nied, P. Oña-Burgos, W. Klopper, F. Breher, *Organometallics* **2011**, *30*, 1419–1428; c) Y. Ito, V. Y. Lee, H. Gornitzka, C. Goedecke, G. Frenking, A. Sekiguchi, *J. Am. Chem. Soc.* **2013**, *135*, 6770–6773; d) A. Jana, V. Huch, M. Repisky, R. J. F. Berger, D. Scheschkewitz, *Angew. Chem. Int. Ed.* **2014**, *53*, 3514–3518; *Angew. Chem.* **2014**, *126*, 3583–3588; e) L. Klemmer, V. Huch, A. Jana, D. Scheschkewitz, *Chem. Commun.* **2019**, *55*, 10100–10103.

[15] e.g. a) A. Zinovieva, V. A. Zinovyev, A. V. Nenashev, S. A. Teys, A. V. Dvurechenskii, O. M. Borodavchenko, V. D. Zhivulko, A. V. Mudryi, *Sci. Rep.* **2020**, *10*, 9308; b) E. M. T. Fadaly, A. Dijkstra, J. R. Suckert, D. Ziss, M. A. J. van Tilburg, C. Mao, Y. Ren, V. T. van Lange, K. Korzun, S. Kölling, M. A. Verheijen, D. Busse, C. Rödl, J. Furthmüller, F. Bechstedt, J. Stangl, J. J. Finley, S. Botti, J. E. Heverkort, E. P. A. M. Bakkers, *Nature* **2020**, *580*, 205–209; c) Z. Li, J. Will, P. Dong, D. Yang, *J. Appl. Phys.* **2017**, *121*, 125704.

[16] Deposition Numbers 2015290 (for [**2**·thf]$_2$), 2015289 (for **3**·NHC), 2015291 (for **4**Li·(NHC)$_2$), 2015292 (for **4**[Li·(dme)$_2$]), and 2158863 (for **5**) contain the supplementary crystallographic data for this paper. These data are provided free of charge by the joint Cambridge Crystallographic Data Centre and Fachin-formationszentrum Karlsruhe Access Structures service.

[17] M. J. Frisch et al., Gaussian 09, Revision C.01. Gaussian, Inc.: Wallingford CT, **2009**. For the full reference see Supporting Information.

[18] TURBOMOLE V7.0 2015 a development of University of Karlsruhe and Forschungszentrum Karlsruhe GmbH, 1989–2007; TURBOMOLE GmbH, since **2007**, available from http://www.turbomole.com: Karlsruhe.

[19] A. J. Cohen, P. Mori-Sánchez, W. Yang, *Science* **2008**, *321*, 792–794.